

Effect of crystal-field split-off hole and heavy-hole bands crossover on gain characteristics of high Al-content AlGaIn quantum well lasers

Jing Zhang, Hongping Zhao, and Nelson Tansu

Citation: *Appl. Phys. Lett.* **97**, 111105 (2010); doi: 10.1063/1.3488825

View online: <http://dx.doi.org/10.1063/1.3488825>

View Table of Contents: <http://apl.aip.org/resource/1/APPLAB/v97/i11>

Published by the [American Institute of Physics](#).

Related Articles

Highly tunable whispering gallery mode semiconductor lasers with controlled absorber

Appl. Phys. Lett. **100**, 061112 (2012)

A capillary absorption spectrometer for stable carbon isotope ratio ($^{13}\text{C}/^{12}\text{C}$) analysis in very small samples

Rev. Sci. Instrum. **83**, 023101 (2012)

Enhancement of random lasing assisted by light scattering and resonance energy transfer based on ZnO/SnO nanocomposites

AIP Advances **2**, 012133 (2012)

Ultra-broad spontaneous emission and modal gain spectrum from a hybrid quantum well/quantum dot laser structure

Appl. Phys. Lett. **100**, 041118 (2012)

Time-dynamics of the two-color emission from vertical-external-cavity surface-emitting lasers

Appl. Phys. Lett. **100**, 041114 (2012)

Additional information on *Appl. Phys. Lett.*

Journal Homepage: <http://apl.aip.org/>

Journal Information: http://apl.aip.org/about/about_the_journal

Top downloads: http://apl.aip.org/features/most_downloaded

Information for Authors: <http://apl.aip.org/authors>

ADVERTISEMENT



Effect of crystal-field split-off hole and heavy-hole bands crossover on gain characteristics of high Al-content AlGa_xN quantum well lasers

Jing Zhang,^{a)} Hongping Zhao, and Nelson Tansu^{b)}

Department of Electrical and Computer Engineering, Center for Optical Technologies, Lehigh University, Bethlehem, Pennsylvania 18015, USA

(Received 22 July 2010; accepted 20 August 2010; published online 14 September 2010)

The optical gain characteristics of high Al-content AlGa_xN quantum wells (QWs) are analyzed for deep UV lasers. The effect of crystal-field split-off hole (CH) and heavy-hole (HH) bands crossover on the gain characteristics of AlGa_xN QW with AlN barriers is analyzed. Attributing to the strong transition between conduction-CH bands, the TM spontaneous emission recombination rate is enhanced significantly for high Al-content AlGa_xN QWs. Large TM-polarized material gain is shown as achievable for high Al-content AlGa_xN QWs, which indicates the feasibility of TM lasing for lasers emitting at ~ 220 – 230 nm. © 2010 American Institute of Physics. [doi:10.1063/1.3488825]

Visible III-nitride lasers and light-emitting diodes (LEDs) are important for medical, storage, and illumination applications.^{1–13} In contrast to visible nitride LEDs,^{1–13} advances have only been realized for deep UV LEDs recently.^{14–22} The applications of deep UV lasers cover free space communication and biochemical agent detection. The pursuit of AlGa_xN deep UV lasers is still challenging^{23–29} due to (1) growth challenges of high Al-content AlGa_xN and (2) lack of understanding in gain characteristics of the quantum well (QW) employed for deep UV laser. Recent works have been reported for low^{26–29} and high^{23,30,31} Al-contents AlGa_xN QWs. However, these works were focused on the quantum efficiency of AlGa_xN QWs LEDs.^{14–22,26–29} The pursuit of electrically injected AlGa_xN QWs lasers have been limited to emission wavelength (λ) ~ 320 – 360 nm,^{26–28} while only optically pumped deep UV laser had been realized.²³

Recent theoretical studies have been carried out for analyzing the optical properties of both low Al-content^{32–34} and high Al-content AlGa_xN QWs.³⁵ The studies on the gain characteristics for high Al-content AlGa_xN QWs are still relatively lacking. The improved understanding in the physics of optical gain of high Al-content AlGa_xN QW is important in identifying the limitations and potential solutions for achieving low-threshold and high-efficiency lasers in the deep UV spectral regime ($\lambda \sim 220$ – 300 nm).

In this work, the gain characteristics and polarization properties of high Al-content AlGa_xN QWs active region are calculated and analyzed. The characteristics of the gain and spontaneous emission rate of high Al-content AlGa_xN QWs are compared with those of low Al-content AlGa_xN QWs. The crossover of crystal-field split-off hole (CH) and heavy hole (HH)/light-hole (LH) bands for high Al-content AlGa_xN QWs is found to have significant impact on the gain properties for deep UV active regions.

The optical gain and spontaneous emission properties of the compressively strained Al_xGa_{1-x}N QW with AlN barriers are analyzed. The calculations of the band structures and wave functions for AlGa_xN QWs were carried out by using self-consistent six-band $k \cdot p$ formalism for wurtzite semiconductor taking into account the valence band mixing, strain effect, polarization fields, and carrier screening effect.^{36–39}

The band parameters for the III-nitride alloys utilized in our calculations were obtained from Refs. 39–41.

The valence band-edge energy levels (HH, LH, and CH) for Al_xGa_{1-x}N as a function of Al-content (x) are shown in Fig. 1. For Al_xGa_{1-x}N with $x < 57.2\%$, the band-edge energy levels for HH and LH bands are larger than that of the CH band. The band-edge energy separations between HH/LH bands and CH band reduce with increasing Al-content, and the HH/LH and CH bands have a crossover at $x = 57.2\%$. For Al_xGa_{1-x}N with $x > 57.2\%$, the band-edge energy level of CH band becomes larger than those of HH/LH bands, and this energy separation further increases as the Al-content in AlGa_xN alloy increases. The HH and CH bands crossover is important, as the transition between conduction and CH bands is transverse magnetic (TM)-polarized component.

Figure 2(a) shows the spontaneous emission recombination rate per unit volume (R_{sp}) for 3 nm Al_xGa_{1-x}N QW ($x = 20\%$ – 80%) sandwiched by AlN barrier layers with carrier density (n) of 3×10^{19} cm⁻³ at T=300 K. The spontaneous emission rates (R_{sp}) for low Al-content AlGa_xN QW show dominant transverse-electric (TE) polarization, which is an order of magnitude higher in comparison to that for the TM polarization. Both the TE- and TM-polarized R_{sp} show increasing trend for increasing Al-content, which are attributed primarily to the larger momentum matrix elements for higher Al-content AlGa_xN QWs. The TM-polarized R_{sp} starts to exhibit large increase for $x > \sim 58\%$. For Al_xGa_{1-x}N QW with $x \sim 68\%$, both TE- and TM-polarized components are similar. For high Al-content above 68%, the TM-polarized R_{sp} is

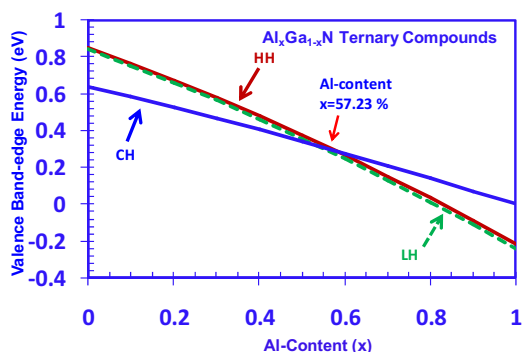


FIG. 1. (Color online) Energy band edges of the HH, LH, and CH bands as a function of Al-content (x) for Al_xGa_{1-x}N ternary compounds.

^{a)}Electronic mail: jiz209@lehigh.edu.

^{b)}Electronic mail: tansu@lehigh.edu.

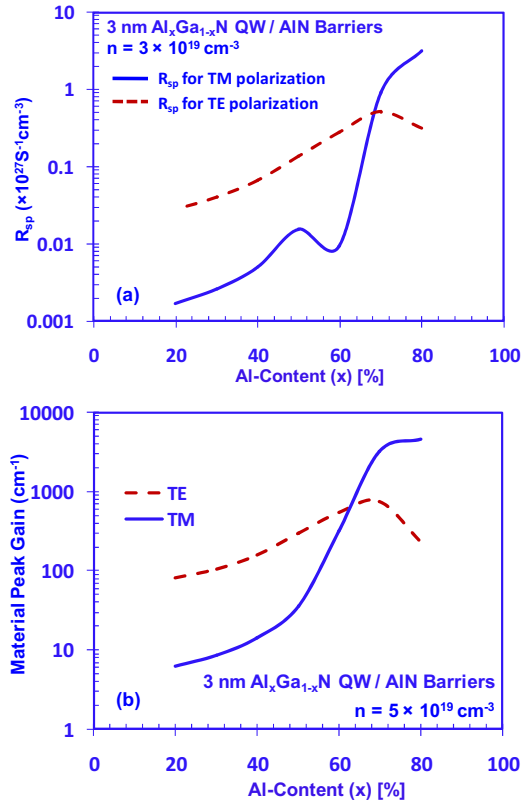


FIG. 2. (Color online) TE- and TM-polarized (a) spontaneous emission rate (R_{sp}) and (b) peak material gain for 3 nm thick $\text{Al}_x\text{Ga}_{1-x}\text{N}$ QWs with AlN barriers as a function of different Al-contents (x).

significantly enhanced attributing to the strong transition between conduction band and CH band. The reduction in the TE-polarized R_{sp} for high Al-content AlGa_N QW can be attributed to the significantly lower carrier density populating the HH and LH bands from the increasing energy separation between CH and HH/LH bands.

Figure 2(b) shows both the TE ($g_{\text{peak}}^{\text{TE}}$) and TM peak material gains ($g_{\text{peak}}^{\text{TM}}$) as a function of Al-content for the 3 nm $\text{Al}_x\text{Ga}_{1-x}\text{N}$ QW with AlN barriers calculated for $n = 5 \times 10^{19} \text{cm}^{-3}$ at $T = 300 \text{K}$. For $\text{Al}_x\text{Ga}_{1-x}\text{N}$ QW with $x < 68\%$, both the $g_{\text{peak}}^{\text{TE}}$ and $g_{\text{peak}}^{\text{TM}}$ are relatively low ($g_{\text{peak}} < 500 \text{cm}^{-1}$), however the $g_{\text{peak}}^{\text{TE}}$ is relatively larger than the $g_{\text{peak}}^{\text{TM}}$. For $\text{Al}_x\text{Ga}_{1-x}\text{N}$ QW with $x > 68\%$, the $g_{\text{peak}}^{\text{TM}}$ is dominant resulting in significantly higher peak gain ($g_{\text{peak}}^{\text{TM}} = 3280 \text{cm}^{-1}$ for $x = 70\%$, and $g_{\text{peak}}^{\text{TM}} = 4690 \text{cm}^{-1}$ for $x = 80\%$). The gain analysis indicates that the carriers in the high Al-content AlGa_N QW are dominantly confined in the CH band after the crossover of the HH/LH and CH bands, resulting in higher than one-order of magnitude ratio of $g_{\text{peak}}^{\text{TM}}/g_{\text{peak}}^{\text{TE}}$ ratio.

Figure 3(a) illustrates the spontaneous emission recombination rate per unit volume (R_{sp}) for 3 nm thick $\text{Al}_x\text{Ga}_{1-x}\text{N}$ QW sandwiched by AlN barrier layers with carrier density (n) up to $n = 6 \times 10^{19} \text{cm}^{-3}$. The analysis was carried out for AlGa_N QW with $x = 60\% - 80\%$. For the $\text{Al}_{0.7}\text{Ga}_{0.3}\text{N}$ QW (or $\text{Al}_{0.8}\text{Ga}_{0.2}\text{N}$ QW), the increase in the spontaneous emission rate (R_{sp}) as a function of carrier density ranges between 3.4–3.9 times (or 5.4–10.5 times) higher compared to that of the $\text{Al}_{0.6}\text{Ga}_{0.4}\text{N}$ QW. The enhancements of the R_{sp} for high Al-content ($x = 70\%, 80\%$) AlGa_N QWs are attributed to the increase in the TM-polarized spontaneous emission rate for AlGa_N QW with Al-content above $\sim 68\%$.

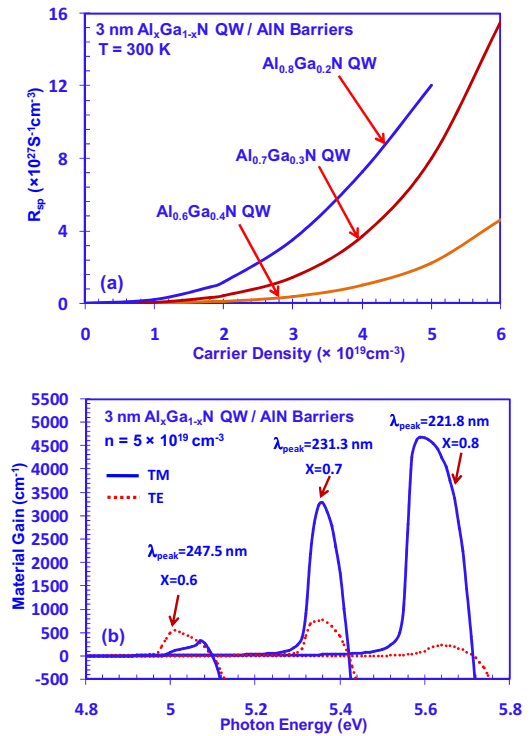


FIG. 3. (Color online) (a) Spontaneous emission radiative recombination rate (R_{sp}) as a function of carrier density, and (b) TE-polarized and TM-polarized optical gain spectra for 3 nm $\text{Al}_x\text{Ga}_{1-x}\text{N}$ QWs with AlN barriers with $x = 60\%, 70\%$, and 80% .

Figure 3(b) shows the TE- and TM-polarized optical gain spectra for $\text{Al}_x\text{Ga}_{1-x}\text{N}$ QWs with $x = 60\% - 80\%$. The peak gain wavelengths (λ_{peak}) for $\text{Al}_x\text{Ga}_{1-x}\text{N}$ QW with $x = 60\%, 70\%$, and 80% are 247.5 nm, 231.3 nm, and 221.8 nm, respectively. For $\text{Al}_{0.6}\text{Ga}_{0.4}\text{N}$ QW, both the TE- and TM-polarized gains are relatively low ($\sim 400 - 500 \text{cm}^{-1}$). However, for the case of higher Al-contents ($x = 70\%, x = 80\%$), the TM-polarized gains increase dramatically, while the TE-polarized gains are significantly lower.

Figures 4(a) and 4(b) show the TM- and TE-polarized material gains ($g_{\text{peak}}^{\text{TM}}$ and $g_{\text{peak}}^{\text{TE}}$) for high Al-content AlGa_N QW as a function of carrier density, respectively. The $g_{\text{peak}}^{\text{TM}}$ for the $\text{Al}_{0.7}\text{Ga}_{0.3}\text{N}$ QW and $\text{Al}_{0.8}\text{Ga}_{0.2}\text{N}$ QW are found to be significantly larger. For $\text{Al}_{0.7}\text{Ga}_{0.3}\text{N}$ QW, the $g_{\text{peak}}^{\text{TM}}$ is 1.5–4.3 times larger than that of the $g_{\text{peak}}^{\text{TE}}$. For $\text{Al}_{0.8}\text{Ga}_{0.2}\text{N}$ QW, the $g_{\text{peak}}^{\text{TM}}$ is $\sim 20 - 110$ times that of the $g_{\text{peak}}^{\text{TE}}$, attributing to its significantly larger energy separation of the CH and HH/LH bands. At $n = 5 \times 10^{19} \text{cm}^{-3}$, the $g_{\text{peak}}^{\text{TM}}$ of $\text{Al}_{0.8}\text{Ga}_{0.2}\text{N}$ QW and $\text{Al}_{0.7}\text{Ga}_{0.3}\text{N}$ QW are 4690cm^{-1} and 3280cm^{-1} , respectively. The $g_{\text{peak}}^{\text{TE}}$ of $\text{Al}_{0.8}\text{Ga}_{0.2}\text{N}$ QW and $\text{Al}_{0.7}\text{Ga}_{0.3}\text{N}$ QW were found as 230cm^{-1} and 765cm^{-1} (at $n = 5 \times 10^{19} \text{cm}^{-3}$), which are relatively negligible compared to the $g_{\text{peak}}^{\text{TM}}$. In contrast to the higher Al-content AlGa_N QWs, the $g_{\text{peak}}^{\text{TE}}$ and $g_{\text{peak}}^{\text{TM}}$ are relatively similar for the $\text{Al}_{0.6}\text{Ga}_{0.4}\text{N}$ QW. The $g_{\text{peak}}^{\text{TE}}$ and $g_{\text{peak}}^{\text{TM}}$ of the $\text{Al}_{0.6}\text{Ga}_{0.4}\text{N}$ QW at $n = 7 \times 10^{19} \text{cm}^{-3}$ are 1425cm^{-1} and 1610cm^{-1} , respectively. Thus, the TM-polarized lasing is feasible for high Al-content AlGa_N QW lasers in the 220–230 nm spectral range.

To analyze the threshold properties of deep UV lasers, AlGa_N QW lasers with optical confinement factor (Γ_{opt}) of 0.02 (Ref. 33) were employed in the analysis. The internal losses (α_i) in typical AlGa_N lasers range from 14cm^{-1} (Ref.

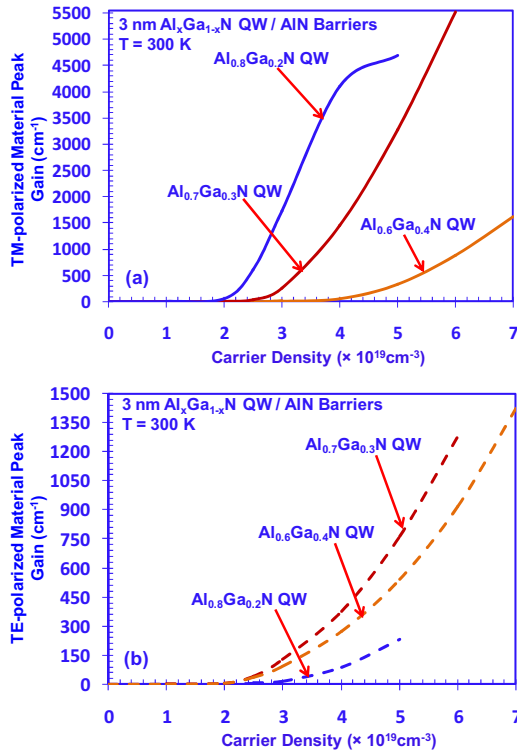


FIG. 4. (Color online) (a) TM-polarized material gain ($g_{\text{peak}}^{\text{TM}}$) and (b) TE-polarized material gain ($g_{\text{peak}}^{\text{TE}}$) as a function of carrier density for 3 nm thick Al_xGa_{1-x}N QWs with AlN barriers with $x=60\%$, 70% , and 80% .

27) up to 50 cm^{-1} .³³ The laser cavity length is assumed as $500 \mu\text{m}$ with end-facet reflectivities of 95% and 35% , which correspond to mirror loss (α_m) of 11 cm^{-1} . The threshold gains (g_{th}) are estimated as $\sim 1250 \text{ cm}^{-1}$ ($\alpha_i=14 \text{ cm}^{-1}$) and $\sim 3050 \text{ cm}^{-1}$ ($\alpha_i=50 \text{ cm}^{-1}$). For the lasers with $g_{th} \sim 1250 \text{ cm}^{-1}$, the threshold carrier densities (n_{th}) are $2.8 \times 10^{19} \text{ cm}^{-3}$ and $3.9 \times 10^{19} \text{ cm}^{-3}$ for Al_{0.8}Ga_{0.2}N QW and Al_{0.7}Ga_{0.3}N QW, respectively. For the lasers with $g_{th} \sim 3050 \text{ cm}^{-1}$, the threshold carrier densities (n_{th}) of $3.5 \times 10^{19} \text{ cm}^{-3}$ and $4.9 \times 10^{19} \text{ cm}^{-3}$ are obtained for Al_{0.8}Ga_{0.2}N QW and Al_{0.7}Ga_{0.3}N QW, respectively.

In summary, the gain characteristics of the high Al-content AlGaIn QWs are analyzed for deep UV lasers. The effect of CH and HH bands crossover on the gain for the AlGaIn QWs for lasers is clarified. After the crossover of the HH/LH and CH bands, the band-edge energy level of CH band is larger than those of the HH/LH bands. The TM-polarized R_{sp} and material gain are dominant for AlGaIn QW with $x > 68\%$. The spontaneous emission rate is significantly enhanced for high Al-content Al_xGa_{1-x}N QW ($x=70\%$, 80%) attributing to the strong transition between conduction band and CH band. The gain analysis shows that large TM-polarized material gain as achievable for high Al-content Al_xGa_{1-x}N QWs, which indicates the feasibility of TM lasing for deep UV lasers emitting at $\sim 220\text{--}230 \text{ nm}$.

This work is supported by National Science Foundation (ECCS Grant No. 0701421), and Class of 1961 Professorship Fund.

¹R. M. Farrell, D. F. Feezell, M. C. Schmidt, D. A. Haeger, K. M. Kelchner, K. Iso, H. Yamada, M. Saito, K. Fujito, D. A. Cohen, J. S. Speck, S. P. DenBaars, and S. Nakamura, *Jpn. J. Appl. Phys., Part 2* **46**, L761 (2007).

²M. H. Kim, M. F. Schubert, Q. Dai, J. K. Kim, E. F. Schubert, J. Piprek,

and Y. Park, *Appl. Phys. Lett.* **91**, 183507 (2007).

³N. Tansu, H. Zhao, G. Liu, X. H. Li, J. Zhang, H. Tong, and Y. K. Ee, *IEEE Photonics Journal* **2**, 236 (2010).

⁴Y. K. Ee, P. Kumnorkaew, R. A. Arif, H. Tong, H. Zhao, J. F. Gilchrist, and N. Tansu, *IEEE J. Sel. Top. Quantum Electron.* **15**, 1218 (2009).

⁵Y. K. Ee, X. H. Li, J. E. Biser, W. Cao, H. M. Chan, R. P. Vinci, and N. Tansu, *J. Cryst. Growth* **312**, 1311 (2010).

⁶S. H. Park, J. Park, and E. Yoon, *Appl. Phys. Lett.* **90**, 023508 (2007).

⁷R. A. Arif, Y. K. Ee, and N. Tansu, *Appl. Phys. Lett.* **91**, 091110 (2007).

⁸R. A. Arif, H. Zhao, and N. Tansu, *IEEE J. Quantum Electron.* **44**, 573 (2008).

⁹H. Zhao, R. A. Arif, and N. Tansu, *IEEE J. Sel. Top. Quantum Electron.* **15**, 1104 (2009).

¹⁰H. Zhao, G. S. Huang, G. Liu, X. H. Li, J. D. Poplawsky, S. Tafon Penn, V. Dierolf, and N. Tansu, *Appl. Phys. Lett.* **95**, 061104 (2009).

¹¹H. Zhao and N. Tansu, *J. Appl. Phys.* **107**, 113110 (2010).

¹²H. Zhao, R. A. Arif, and N. Tansu, *J. Appl. Phys.* **104**, 043104 (2008).

¹³H. Zhao, G. Liu, R. A. Arif, and N. Tansu, *Solid-State Electron.* **54**, 1119 (2010).

¹⁴A. Yasan, R. McClintock, K. Mayes, D. Shiell, L. Gautero, S. R. Darvish, P. Kung, and M. Razeghi, *Appl. Phys. Lett.* **83**, 4701 (2003).

¹⁵A. J. Fischer, A. A. Allerman, M. H. Crawford, K. H. A. Bogart, S. R. Lee, R. J. Kaplar, W. W. Chow, S. R. Kurtz, K. W. Fullmer, and J. J. Figiel, *Appl. Phys. Lett.* **84**, 4762 (2004).

¹⁶V. Adivarahan, S. Wu, J. P. Zhang, A. Chitnis, M. Shatalov, V. Mandavilli, R. Gaska, and M. A. Khan, *Appl. Phys. Lett.* **84**, 3394 (2004).

¹⁷Z. Ren, Q. Sun, S. Y. Kwon, J. Han, K. Davitt, Y. K. Song, A. V. Nurmikko, H. K. Cho, W. Liu, J. A. Smart, and L. J. Schwalter, *Appl. Phys. Lett.* **91**, 051116 (2007).

¹⁸A. V. Sampath, M. L. Reed, C. Chua, G. A. Garrett, G. Dang, E. D. Readinger, H. Shen, A. Usikov, O. Kovalenkov, L. Shapovalova, V. A. Dmitriev, N. M. Johnson, and M. Wraback, *Phys. Status Solidi C* **5**, 2303 (2008).

¹⁹C. G. Moe, M. L. Reed, G. A. Garrett, A. V. Sampath, T. Alexander, H. Shen, M. Wraback, Y. Bilenko, M. Shatalov, J. Yang, W. Sun, J. Deng, and R. Gaska, *Appl. Phys. Lett.* **96**, 213512 (2010).

²⁰Y. Sakai, Y. Zhu, S. Sumiya, M. Miyoshi, M. Tanaka, and T. Egawa, *Jpn. J. Appl. Phys.* **49**, 022102 (2010).

²¹Y. Taniyasu and M. Kasu, *Appl. Phys. Lett.* **96**, 221110 (2010).

²²H. Hirayama, N. Noguchi, and N. Kamata, *Appl. Phys. Express* **3**, 032102 (2010).

²³T. Takano, Y. Narita, A. Horiuchi, and H. Kawanishi, *Appl. Phys. Lett.* **84**, 3567 (2004).

²⁴M. Kneissl, Z. Yang, M. Teepe, C. Knollenberg, O. Schmidt, P. Kiesel, N. M. Johnson, S. Schujman, and L. J. Schowalter, *J. Appl. Phys.* **101**, 123103 (2007).

²⁵V. N. Jmerik, A. M. Mizerov, A. A. Sitnikova, P. S. Kop'ev, S. V. Ivanov, E. V. Lutsenko, N. P. Tarasuk, N. V. Rzhetskii, and G. P. Yablonskii, *Appl. Phys. Lett.* **96**, 141112 (2010).

²⁶H. Yoshida, M. Kuwabara, Y. Yamashita, K. Uchiyama, and H. Kan, *Appl. Phys. Lett.* **96**, 211122 (2010).

²⁷H. Yoshida, M. Kuwabara, Y. Yamashita, Y. Takagi, K. Uchiyama, and H. Kan, *New J. Phys.* **11**, 125013 (2009).

²⁸M. Kneissl, D. W. Treat, M. Teepe, N. Miyashita, and N. M. Johnson, *Appl. Phys. Lett.* **82**, 25 (2003).

²⁹C. Chen, M. Shatalov, E. Kuokstis, V. Adivarahan, M. Gaevski, S. Rai, and M. Asif Khan, *Jpn. J. Appl. Phys., Part 2* **43**, L1099 (2004).

³⁰T. M. Al Tahtamouni, N. Nepal, J. Y. Lin, H. X. Jiang, and W. W. Chow, *Appl. Phys. Lett.* **89**, 131922 (2006).

³¹K. B. Nam, J. Li, M. L. Nakarmi, J. Y. Lin, and H. X. Jiang, *Appl. Phys. Lett.* **84**, 25 (2004).

³²W. W. Chow, M. Kneissl, J. E. Northrup, and N. M. Johnson, *Appl. Phys. Lett.* **90**, 101116 (2007).

³³W. W. Chow and M. Kneissl, *J. Appl. Phys.* **98**, 114502 (2005).

³⁴S. H. Park and S. L. Chuang, *Appl. Phys. A: Mater. Sci. Process.* **78**, 107 (2004).

³⁵S. H. Park, *Semicond. Sci. Technol.* **24**, 035002 (2009).

³⁶S. L. Chuang, *IEEE J. Quantum Electron.* **32**, 1791 (1996).

³⁷S. L. Chuang and C. S. Chang, *Semicond. Sci. Technol.* **12**, 252 (1997).

³⁸S. L. Chuang, *Physics of Photonic Devices*, 2nd ed. (Wiley, New York, 2009, Chap. 4).

³⁹H. Zhao, R. A. Arif, Y. K. Ee, and N. Tansu, *IEEE J. Quantum Electron.* **45**, 66 (2009).

⁴⁰I. Vurgaftman and J. R. Meyer, in *Nitride Semiconductor Devices*, edited by J. Piprek (Wiley, New York, 2007), Chap. 2.

⁴¹I. Vurgaftman and J. R. Meyer, *J. Appl. Phys.* **94**, 3675 (2003).